Solid State Communications 150 (2010) 655–659

Contents lists available at ScienceDirect

Solid State Communications

journal homepage: www.elsevier.com/locate/ssc

Effect of a gap opening on the conductance of graphene superlattices

M. Esmailpour [a], A. Esmailpour [b,c], Reza Asgari [c,*], M. Elahi [a], M.R. Rahimi Tabar [d,e]

[a] Department of Physics, Razi University, Kermanshah, Iran
[b] Department of Physics, Shahid Rajaei University, Lavizan, Tehran 16788, Iran
[c] School of Physics, Institute for Fundamental Sciences, (IPM) Tehran 19395-5531, Iran
[d] Department of Physics, Sharif University of Technology, 11365-9161, Tehran, Iran
[e] Institute of Physics, Carl von Ossietzky University, D-26111 Oldenburg, Germany

ARTICLE INFO

Article history:
Received 16 July 2009
Received in revised form
5 October 2009
Accepted 17 December 2009
by V. Pellegrini
Available online 23 December 2009

Keywords:
A. Graphene
A. Nanostructures
D. Electronic transport
D. Tunneling

ABSTRACT

The electronic transmission and conductance of a gapped graphene superlattice were calculated by means of the transfer-matrix method. The system that we study consists of a sequence of electron-doped graphene as wells and hole-doped graphene as barriers. We show that the transmission probability approaches unity at some critical value of the gap. We also find that there is a domain around the critical gap value for which the conductance of the system attains its maximum value.

1. Introduction

Graphene, a single atomic layer of crystalline carbon on the honeycomb lattice that consists of two interpenetrating triangular sublattices A and B, has opened up a new field for fundamental studies and applications [1–5]. Peculiar electronic properties of graphene give rise to the possibility of overcoming the limitations of the silicon-based electronic structure [6]. The electronic spectrum in graphene contains two zero energy at K^+ and K^- points of the Brillouin zone, which are called the valleys or Dirac points. The massless Dirac-like carriers in graphene have almost semi-ballistic transport behavior with small resistance, due to the suppression of the back-scattering process [7]. The mobility of the carriers in graphene is quite high [8–11] and is much higher than the electron mobility revealed in the semiconductor hetrostructures [12,13].

In graphene sheets the type of particle (electrons or holes) and the density of the carriers can be controlled by tuning a gate bias voltage [2,14,15]. In a gapless graphene electrical conduction cannot be switched off by using the control voltages [16], which is essential for the operation of conventional transistors. One can overcome such difficulties by generating a gap in the electronic spectrum. The band gap is a measure of the threshold voltage and the on–off ratio of the field effect transistors [17,18]. Therefore, it is essential to induce a band gap at the Dirac points in order to control the transport of the carriers and integrating graphene into the semiconductor technology. Consequently, band gap engineering in graphene is a current topic of much interest with fundamental and applied significance [19].

In the literature several routes have been proposed and applied to induce and to control a gap in graphene. One of them is using quantum-confined geometries, such as quantum dots or nanoribbons [20–24]. It has been shown that the gap values increase by decreasing the nanoribbon width. An alternative way is spin–orbit coupling whose origin is due to both intrinsic spin–orbit interactions, or the Rashba interaction [25–28]. Yet another method to generate a gap in graphene sheets is through an inversion symmetry breaking of the sublattice, when the number of the electrons on A and B atoms are different [29–32], e.g., graphene placement on proper substrates [33–40].

Graphene superlattices, on the other hand, may be fabricated by adsorbing adatoms on the graphene surface by positioning and aligning impurities with scanning tunneling microscopy [41], or by applying a local top gate voltage to graphene [42]. The transition of hitting massless particles in a clean [43] or disordered [44] graphene-based superlattice structure has been studied. It is shown that the conductivity of the system depends on the superlattice structural parameters. Furthermore, the superlattice

* Corresponding author. Tel.: +98 21 22280692; fax: +98 21 22280415.
E-mail address: asgari@theory.ipm.ac.ir (R. Asgari).

0038-1098/$ – see front matter
doi:10.1016/j.ssc.2009.12.024

structure of the graphene nanoribbons was recently studied by using first-principle density-functional theory calculations [45]. These calculations showed that the magnetic ground state of the constituent ribbons, the symmetry of the junction, and their functionalization by adatoms represent structural parameters to the electronic and magnetic properties of such structures. It would, therefore, be worthwhile to investigate how the conductance of graphene superlattice junctions is affected by a gap opening at the Dirac points.

In this paper we consider the sublattice symmetry-breaking mechanism due to the fact that the densities of the particles associated with the on-site energy for A and B sublattices are different or, equivalently, consider the intrinsic spin–orbit interaction for a gap opening in a clean graphene superlattice. We investigate the transmission probability of the Dirac fermions through the system. In the cases of a single barrier and double barrier, exact analytical analyses are carried out for calculating the transmission probability. In addition, we show that the group delay time is different from the dwell time for a system that consists of a gap opening.

The rest of the paper is organized as follows. The theory and method are discussed in Section 2. The numerical results and discussions are given in Section 3. A brief summary is given in Section 4.

2. The superlattice model

We consider a graphene with a peculiar gap opening due to the sublattice symmetry breaking, where the 2D massive Dirac fermions at low energy are described by noninteracting Hamiltonian [46] $\widehat{H} = \hbar v_F \sigma \cdot \mathbf{k} + m v_F^2 \sigma_z$. There are two eigenvalues $\pm E_k$, where $E_k = \sqrt{\hbar^2 v_F^2 k_F^2 + \Delta^2}$ is the particle dispersion relation with energy gap $\Delta = m v_F^2$. Moreover, the Fermi velocity, $v_F \approx 10^6$ ms^{-1}, the Fermi momentum of electron is k_F and σ_i, where $i = x, y$ and z, are Pauli matrices. We consider a sequence of electron doped-graphene as wells, and hole-doped graphene as barriers, a schematic of which with the associated potential is illustrated in Fig. 1. The growth direction is taken to be the x axis, which is designed as the superlattice axis. The coordinate of the ith interface is labeled by l_i where, $l_i = \text{integer}[\frac{i}{2}]D + \text{integer}[\frac{i-1}{2}]L$. The schematic diagram of the electronic spectrum of the gapped graphene is shown in Fig. 1 (top graph) as well. Due to the difference between the Fermi energy and the band structure between two graphene strips, the potential profile of the system is the multiple quantum well structure which is described by

$$V(x) = \begin{cases} V_0, & \text{if } l_{2i-1} < |x| < l_{2i}; \\ 0, & \text{otherwise.} \end{cases} \tag{1}$$

To solve the transport problem in a graphene superlattice, we assume that the incident electron propagates at angle ϕ along the x axis (see Fig. 1) with energy $E = 2\pi v_F/\lambda$, and with the wavelength λ across the barriers, in such a way that the Fermi level lies in the conduction band outside the barrier and the valence band inside it. Throughout the paper, we consider the Klein zone in which $\Delta < E < V_0 - \Delta$. The Dirac spinor components that are the solutions to the Dirac Hamiltonian are expressed as

$$\psi_1(x, y) = (a_i e^{ik_{ix}x} + b_i e^{-ik_{ix}x}) e^{ik_y y}$$
$$\psi_2(x, y) = s_i (a_i e^{ik_{ix}x + i\varphi_i} - b_i e^{-ik_{ix}x - i\varphi_i}) e^{ik_y y} \tag{2}$$

where a_i and b_i are the transmission amplitudes. Here $s_i = sgn(E - V(x))$, $k_x^2 = (E^2 - \Delta^2)/\hbar^2 v_F^2 - k_{iy}^2$, and, $q_x^2 = ((E - V_0)^2 - \Delta^2)/\hbar^2 v_F^2 - k_y^2$, with, k_{ix} being k_x or q_x. Moreover, φ_i is either ϕ or θ for the well and the barrier, respectively. $k_x = k_F \cos\phi$ and $k_y = k_F \sin\phi$ are the wave vector components for the outside region of the barriers.

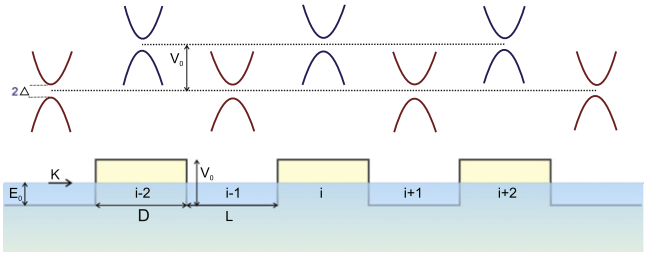

Fig. 1. Model of gapped graphene superlattices.

To calculate the transmission coefficients, we use the transfer-matrix method. To this end, we apply the continuity of the wave functions at the boundaries and construct the transfer matrices as follows:

$$\begin{pmatrix} 1 \\ r \end{pmatrix} = \frac{1}{\sin(\alpha_k)\cos(\phi_i)} M S(x) \mathcal{N} a_N \tag{3}$$

where

$$M = \begin{pmatrix} \rho_2\eta_1 e^{-i\phi} - \rho_1\eta_2 e^{i\theta} & \rho_2\eta_1 e^{-i\phi} - \rho_1\eta_2 e^{-i\theta} \\ \rho_2\eta_1 e^{i\phi} - \rho_1\eta_2 e^{i\theta} & \rho_2\eta_1 e^{i\phi} - \rho_1\eta_2 e^{-i\theta} \end{pmatrix},$$
$$\mathcal{N} = \begin{pmatrix} e^{ik_x l_N}\left(\frac{\rho_1}{\rho_2}e^{-i\theta} - \frac{\eta_1}{\eta_2}e^{i\phi}\right) \Big/ [2e^{iq_x l_N}\cos\theta] \\ e^{ik_x l_N}\left(\frac{\rho_1}{\rho_2}e^{i\theta} + \frac{\eta_1}{\eta_2}e^{i\phi}\right) \Big/ [-2e^{iq_x l_N}\cos\theta] \end{pmatrix}$$
$$s(x = l_i) = \begin{pmatrix} t_{11} & t_{12} \\ t_{21} & t_{22} \end{pmatrix}, \qquad S(x) = s(l_2)s(l_3)\ldots s(l_{N-1}) \tag{4}$$

and r and a_N are the reflection and the transmission coefficients of the system that consists of N barriers. We have defined parameters $\rho_1 = \cos(\alpha_k/2)$, $\eta_1 = \sin(\alpha_k/2)$, $\rho_2 = \sin(\acute{\alpha}_k/2)$, and, $\eta_2 = \cos(\acute{\alpha}_k/2)$. The angles α_k and $\acute{\alpha}_k$ are determined by $\tan(\alpha_k) = \hbar v_F (k_x^2 + k_y^2)^{\frac{1}{2}}/\Delta$ and $\tan(\acute{\alpha}_k) = \hbar v_F (q_x^2 + k_y^2)^{\frac{1}{2}}/\Delta$, respectively. The elements of s matrix have the form

$$t_{11} = e^{i(k_{ix} - k_{(i-1)x})l_{i-1}}\left[-\frac{\eta_i}{\eta_{i-1}}e^{i\varphi_i} + \frac{\rho_i}{\rho_{i-1}}e^{-i\varphi_{i-1}}\right] \Big/ 2\cos(\varphi_{i-1}) \tag{5}$$
$$t_{12} = e^{i(-k_{ix} - k_{(i-1)x})l_{i-1}}\left[\frac{\eta_i}{\eta_{i-1}}e^{-i\varphi_i} + \frac{\rho_i}{\rho_{i-1}}e^{-i\varphi_{i-1}}\right] \Big/ 2\cos(\varphi_{i-1})$$
$$t_{21} = e^{i(k_{ix} + k_{(i-1)x})l_{i-1}}\left[-\frac{\eta_i}{\eta_{i-1}}e^{i\varphi_i} + \frac{\rho_i}{\rho_{i-1}}e^{i\varphi_{i-1}}\right] \Big/ 2\cos(\varphi_{i-1})$$
$$t_{22} = e^{i(-k_{ix} + k_{(i-1)x})l_{i-1}}\left[-\frac{\eta_i}{\eta_{i-1}}e^{-i\varphi_i} + \frac{\rho_i}{\rho_{i-1}}e^{i\varphi_{i-1}}\right] \Big/ 2\cos(\varphi_{i-1}).$$

The angle dependence of the transmission probability $T = |a_N|^2$ is obtained by solving Eq. (3) for a given N. It should be noted that the transmission coefficients for the gapless graphene [44] is revealed by setting $\Delta = 0$ in Eqs. (2)–(5). After the transmission coefficients are obtained, the conductivity of the system is computed by means of the Büttiker formula [47], taking the integral of $T(E, \phi)$ over the angle,

$$G = G_0 \int_{-\frac{\pi}{2}}^{\frac{\pi}{2}} T(E, \phi)\cos(\phi) d\phi \tag{6}$$

where $G_0 = e^2 m_e v_F w/\hbar^2$ with w being the width of the graphene strip along the y direction.

2.1. Exact analysis for single- and double-barrier systems

Let us first consider a system composed of a single barrier. The wave functions in the different regions can be written as

$$\psi_1(x,y) = e^{(ixk_x+yk_y)}\begin{pmatrix}\rho_1\\ e^{i\phi}s\eta_1\end{pmatrix} + re^{i(-xk_x+yk_y)}\begin{pmatrix}\rho_1\\ e^{i(\pi-\phi)}s\eta_1\end{pmatrix}$$

$$\psi_2(x,y) = ae^{i(xq_x+yk_y)}\begin{pmatrix}\rho_2\\ e^{i\theta}s'\eta_2\end{pmatrix} + be^{-i(xq_x+yk_y)}\begin{pmatrix}\rho_2\\ e^{i(\pi-\phi)}s'\eta_2\end{pmatrix}$$

$$\psi_3(x,y) = te^{i(xk_x+yk_y)}\begin{pmatrix}\rho_1\\ e^{i\theta}s\eta_1\end{pmatrix}. \quad (7)$$

It should be noted that since the interface is located along the y, due to the conservation of the momentum we have, $k_y = q_y$. After some straightforward calculations, the electronic transmission probability, $T(\phi)$, through the barrier is obtained, resulting in

$$T(\phi) = \frac{\cos^2\theta\cos^2\phi}{\cos^2\phi\cos^2\theta\cos^2 Dq_x + \sin^2 Dq_x\left(\sin\phi\sin\theta + \frac{C}{2B}\right)^2} \quad (8)$$

where $C/B = \tan\alpha_k/2\tan\alpha_{k'}/2 + \cot\alpha_k/2\cot\alpha_{k'}/2$.

It is useful to investigate the conditions under which the transmission probability approaches unity. We find from Eq. (8) that when $Dq_x = n\pi$ (n is an integer), the barrier becomes entirely transparent and does not depend on the parameter ϕ. The same condition at the normal incidence was obtained in [48].

For a double-barrier system, the calculation of the transmission would be difficult. In this case we restrict the calculations to the case, $\phi = 0$. The electronic transmission expression for the double-barrier system at normal incidence takes the form

$$T(\phi = 0) = \frac{64(\rho_1\eta_1\rho_2\eta_2)^4}{A^2\cos^2(2q_xD) + P + Q + Z} \quad (9)$$

where $A = 6(\rho_1\eta_1\rho_2\eta_2)^2 + (\eta_1\rho_2)^4 + (\rho_1\eta_2)^4$, $B = 2(\rho_1\eta_1\rho_2\eta_2)^2 - (\eta_1\rho_2)^4 - (\rho_1\eta_2)^4$, $C = \rho_1\eta_1^3\rho_2^3\eta_2 + \rho_1^3\eta_1\rho_2\eta_2^3$, $P = 16C^2\sin^2(2q_xD) + 8BC\sin(2k_xL)\sin(2q_xD)(\cos(2q_xD) - 1)$, $Q = B^2[1 + 2\cos(2k_xL)(\cos(2q_xD) - 1) + (1 - \cos(2q_xD))^2]$ and $Z = 2AB\cos(2q_xD)[1+(\cos(2q_xD)-1)\cos(2k_xL)]$. In the numerical section below, we find some critical gap values for which $T(\phi = 0) = 1$ and show that the critical points are in good agreement with the results calculated by the analytical expressions.

2.2. The Hartman effect in a gapped graphene

In this section we study tunneling through the single barrier and calculate two important tunneling times, the group delay time τ_g and the dwell time τ_d [49]. The relationship between the two times was first studied by Winful [50] for a one-dimensional electron gas system. It was shown that there is a difference between the two times in the conventional electron gas systems. Using the energy derivative of the transmission phase shift [50], the group delay time is obtained through $\tau_{gt} = \hbar d\phi_0/dE$, where $\phi_0 = \phi_t + k_xD$, and the group delay time in reflection is given by $\tau_{gr} = \hbar d\phi_r/dE$. Here, ϕ_i ($i = t$ or r) denotes the phase angle of the transmission or the reflection wave function.

For a general asymmetric barrier, τ_{gt} differs from τ_{gr}, and the group delay time τ_g is obtained by $\tau_g = |t^2|\tau_{gt}+|r^2|\tau_{gr}$, whereas for symmetric barriers, $\tau_g = \tau_{gt} = \tau_{gr}$. The dwell time—the time spent by a particle in the barrier—is expressed as, $\tau_d = \int_0^D |\psi(x)|^2 dx/j_{in}$, where $\psi(x)$ is the stationary state wave function with energy E, with $j_{in} = v_F\cos(\phi)$ being the flux of the incident particles. According to calculations given in [51], we have

$$\int_0^D |\psi(x)|^2 dx = -i\hbar v_F[(\psi^\dagger(r)\sigma_x\partial_E\psi(r))_{x=D} - (\psi^\dagger(r)\sigma_x\partial_E\psi(r))_{x=0}]. \quad (10)$$

For the system, the wave functions are described by

$$\psi_1(x,y) = e^{(ixk_x+yk_y)}\begin{pmatrix}\rho_1\\ e^{i\phi}s\eta_1\end{pmatrix} + re^{i(-xk_x+yk_y)}\begin{pmatrix}\rho_1\\ e^{i(\pi-\phi)}s\eta_1\end{pmatrix} \quad (11)$$

in front of the barrier and

$$\psi_3(x,y) = te^{i(xk_x+yk_y)}\begin{pmatrix}\rho_1\\ e^{i\phi}s\eta_1\end{pmatrix} \quad (12)$$

for behind the barrier. Therefore, the right-hand side of Eq. (10) becomes $2v_F\rho_1\eta_1\cos\phi\{|t|^2\hbar d\phi_0/dE + |r|^2\hbar d\phi_r/dE\}$. Consequently, the relationship between τ_d and τ_g is obtained by

$$\tau_d = \frac{\varepsilon_k}{\sqrt{{\varepsilon_k}^2 + \Delta^2}}\tau_g. \quad (13)$$

The τ_g differs from the τ_g and they are no longer the same in the presence of the gap values. Note that the energy of a quasiparticle is $\varepsilon_k = \hbar v_F|\overrightarrow{k}|$. The dwell time becomes equal to the group delay time by setting $\Delta = 0$. The last result is in contrast to the result obtained for a conventional 2D electron gas system, where the dwell time equals the group delay time plus a self interference term, which comes from the overlap of the incident and reflected waves in front of the barrier.

3. Numerical results and discussion

We evaluated the electronic transmission probability and conductance in the gapped graphene through a finite number of potential barriers, as a function of the gap value introduced in the system. In all of the numerical calculations we assumed that the wavelength of the incident electron is $\lambda = 50$ nm and $V_0 = 200$ meV. In all the figures Δ scales in meV.

We first calculated the transmission probability of the charge carriers through the graphene structure with a double barrier, $N = 2$, with the barrier width $D = 50$ nm. Fig. 2 shows the transmission probability of the incident electrons hitting a graphene superlattice as a function of the angle ϕ for several values of the gap values, Δ, with (a) $L = 50$ nm and (b) $L = 70$ nm, respectively. The magnitude of T behaves non-monotonically with the increase of the energy gap value at $\phi = 0$. It shows that the Klein tunneling is no longer applicable when there is a band gap in graphene. It should be noted that the Kelin tunneling predicts that the chiral massless carrier can pass through a high electrostatic potential barrier with probability one, regardless of the height and width of the barrier at normal incidence. In addition, to verify the dependence on the well width of the transmission probability, we calculated the electronic transmission for the several values of the parameter L. The results are depicted in Fig. 2(b).

To verify the behavior of the electronic transmission probability at normal incidence, the calculated transmission probability as a function of the band gap value for the several numbers of the potential barriers is shown in Fig. 3(a). The structural parameters are the same as in Fig. 2(a). The results for a single barrier, $N = 1$, show that when Δ increases, the transmission probability exhibits a minimum at $\Delta \simeq 62$ meV, and then it reaches unity at the critical value given by $\Delta_c = 82$ meV. The critical gap values entirely coincide with the results calculated analytically. In the case of $\phi = 0$, we found analytically that $\Delta_c = \sqrt{(E - V_0)^2 - (\hbar v_F)^2(n\pi/D)^2}$, which is supported by the numerical calculations.

In the case of the double barrier, $N = 2$, there are three Δ_c values with which T becomes exactly unity. For the system that consists of an even number of the potential barriers, we found that the superlattice is fully transparent ($T = 1$), when the energy gap is $\Delta_c = 53.5$ meV. Note that the critical value of the band gap Δ_c depends on the superlattice structural parameters, as we show numerically in Fig. 3(b), where $L = 70$ nm. The number of

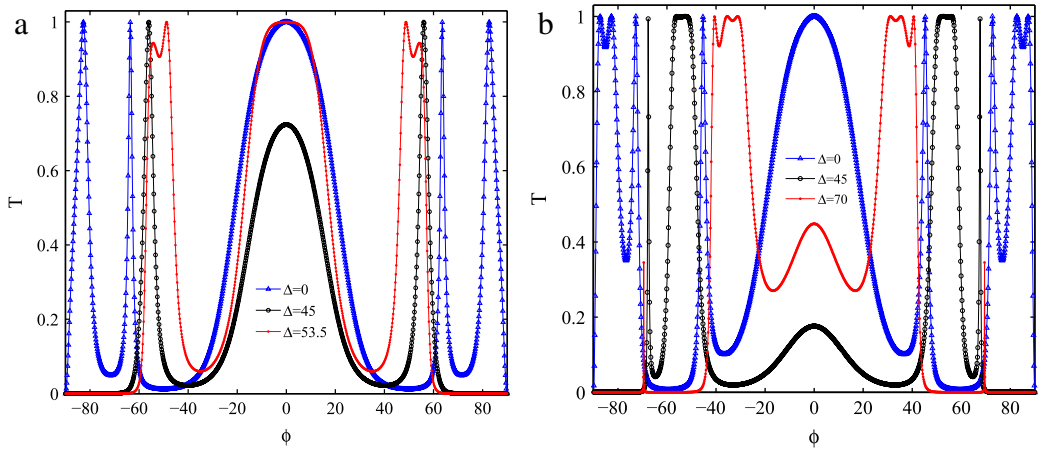

Fig. 2. Transmission probability T of the electrons through the double-barrier structures as a function of the incident angle and the parameter Δ. The value of the barrier width is $D = 50$ nm and those of the well width are (a) $L = 50$ nm, and (b) 70 nm.

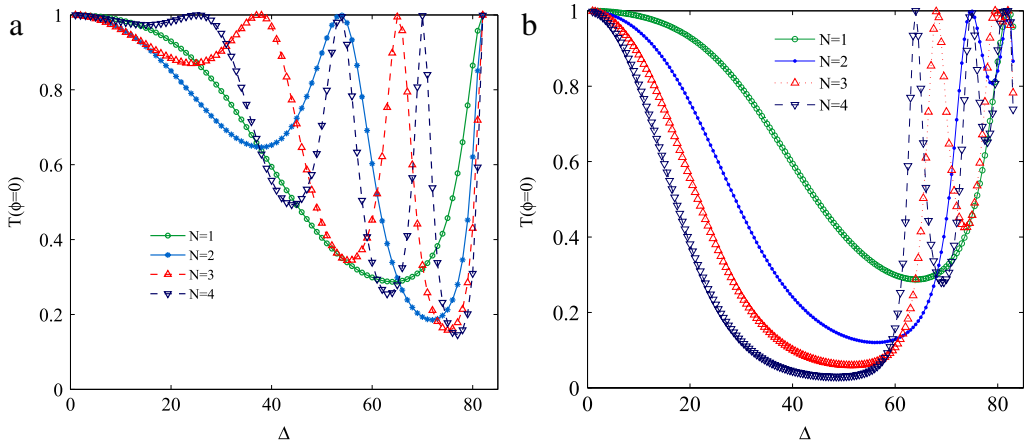

Fig. 3. Transmission probability T for the normal incident electrons through graphene superlattice as a function of Δ for (a) $L = 50$ nm, and (b) $L = 70$ nm for several numbers of the barriers.

the maxima at which the transmission amplitude becomes unity increases with the increasing number of the potential barriers.

We also studied that how the structural parameters affect the transmission of the system. Fig. 4 presents $T(\phi = 0)$ as a function of the well width for the several values of the barrier width. The number of the potential barriers is $N = 2$, and the value of gap was chosen as $\Delta = 53.5$ meV. The numerically calculated $T(\phi = 0)$ is in good agreement with the result obtained analytically using Eq. (9). Furthermore, the transmission probability approaches unity only for the specific values, $L = 0, 25, 50, 75, 100, \ldots$ at $D = 50$ meV. However, when $D = 20$ or 80 meV, the transmission probability is independent of the parameter L at normal incidence angle, and always approaches unity. The numerical results predict the transmission probability at normal incidence angle to be unity for the case that $2q_xD = 2n\pi$ and that is independent of L. However, when $2q_xD = (2n-1)\pi$, the transmission probability would be unity if $2k_xL = 2m\pi$. Therefore, the transmission probability depends strongly on the structural parameters in the gapped graphene superlattice.

Finally, we calculated the electronic conductance as a function of Δ for the various numbers of the potential barriers. The results are shown in Fig. 5. Finite-size scaling analysis indicates that G tends to a nonzero constant at $\Delta = 80$ meV. Moreover, there is a domain value of Δ for which the conductivity attains its maximum value. According to the above discussions, it is clear that the conductivity of the system depends on the superlattice structural parameters, such as L and D. Importantly, we would like

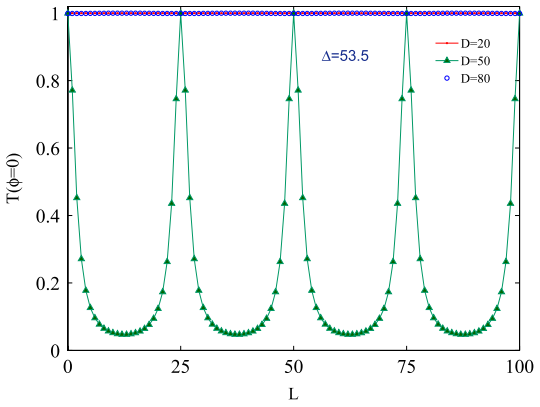

Fig. 4. Transmission probability T for the normal incident electrons through the graphene superlattice that consist of $N = 2$ as a function of well's width L at $\Delta = 53.5$ meV for several values of the barrier width D.

to stress that the electronic conductance can reach a maximum value by selecting the proper gap and the barrier width.

4. Summary

We evaluated the electronic conductance in gapped graphene with a finite number of potential barriers. An exact analytic expression was derived for the electronic transmission probability in a system with a single or two barrier, and the critical values

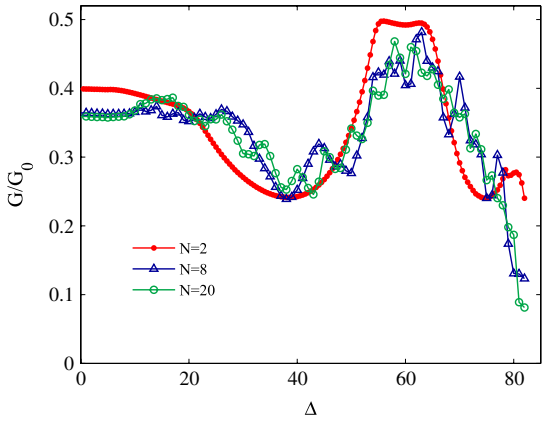

Fig. 5. Conductance of the graphene superlattice as a function of the parameter Δ for $L = 50$ nm and several numbers of the barriers.

of the gap at which the transmission probability equals unity were computed. We showed that the group delay time is not the same as the dwell time in a gapped graphene that consists of a barrier. However, they are the same in a gapless graphene. It should be noted that the extension of the dwell time for a superlattice structure needs intensive computations and will be reported in future. Moreover, we showed that the conductance can attain its maximum for a domain value of gaps around the critical value. In addition, the conductance of the system depends on the superlattice structural parameters and, therefore, one may design a very good electronic device by selecting the proper gap and the barrier width. Thus, the system with a proper arrangement might be of use in electronic or electromagnetic devices. Finally, the present calculations may be improved to investigate the spin dependence of the conductance.

Acknowledgements

We are grateful to M. Sahimi who carefully read the manuscript. A.E. acknowledges supporting from the SRU.

References

[1] K.S. Novoselov, A.K. Geim, S.V. Morozov, D. Jiang, Y. Zhang, S.V. Dubonos, I.V. Grigorieva, A.A. Firsov, Science 306 (2004) 666.
[2] K.S. Novoselov, A.K. Geim, S.V. Morozov, D. Jiang, M.I. Katsnelson, I.V. Grigorieva, S.V. Dubonos, A.A. Firsov, Nature 438 (2005) 197.
[3] K.S. Novoselov, D. Jiang, F. Schedin, T.J. Booth, V.V. Khotkevich, S.V. Morozov, A.K. Geim, Proc. Natl. Acad. Sci. 102 (2005) 10451.
[4] Y. Zhang, Y. Tan, H.L. Stormer, P. Kim, Nature 438 (2005) 201.
[5] A.K. Geim, Science 324 (2009) 1530.
[6] P. Avouris, Z. Chen, V. Perebeinos, Nature Nanotechnol. 2 (2007) 605.
[7] A.A. Balandin, S. Ghosh, W. Bao, I. Calizo, D. Teweldebrhan, F. Miao, C.N. Lau, Nano Lett. 8 (2008) 902.
[8] S.V. Morozov, K.S. Novoselov, M.I. Katsnelson, F. Schedin, D.C. Elias, J.A. Jaszczak, A.K. Geim, Phys. Rev. Lett. 100 (2008) 016602.
[9] K.I. Bolotin, K.J. Sikes, J. Hone, H.L. Stormer, P. Kim, Phys. Rev. Lett. 101 (2008) 096802.
[10] X. Du, I. Skachko, A. Barker, E.Y. Andrei, Nature Nanotechnol. 3 (2008) 491.
[11] K.I. Bolotin, K.J. Sikes, Z. Jiang, M. Klima, G. Fudenberg, J. Hone, P. Kim, H.L. Stormer, Solid State Commun. 146 (2008) 351.
[12] K. Eng, R.N. McFarland, B.E. Kane, Appl. Phys. Lett. 87 (2005) 052106.
[13] E.H. Hwang, S. Das Sarma, Phys. Rev. B 75 (2007) 073301.
[14] Y.B. Zhang, Y.W. Tan, H.L. Stormer, P. Kim, Nature 438 (London) (2005) 201.
[15] J. Nilsson, A.H. Castro Neto, F. Guinea, N.M.R. Peres, Phys. Rev. B 76 (2007) 165416.
[16] M.I. Katsnelson, K.S. Novoselov, A.K. Geim, Nature Phys. 2 (2006) 620.
[17] Y. Lin, K.A. Jenkins, A. Valdes-Garcia, J.P. Small, D.B. Farmer, P. Avouris, Nano Lett. 9 (2009) 422.
[18] J. Kedzierski, P. Hsu, P. Healey, P.W. Wyatt, C.L. Keast, M. Sprinkle, C. Berger, W.A. de Heer, IEEE Trans. Electron Devices 55 (2008) 2078.
[19] K. Novoselov, Nature Mater. 6 (2007) 720.
[20] Y.W. Son, M.L. Cohen, S.G. Louie, Phys. Rev. Lett. 97 (2006) 216803.
[21] M.Y. Han, B. Ozyilmaz, Y. Zhang, P. Kim, Phys. Rev. Lett. 98 (2007) 206805.
[22] L. Yang, C.-H. Park, Y.-W. Son, M.L. Cohen, S.G. Louie, Phys. Rev. Lett. 99 (2007) 186801.
[23] D. Finkenstadt, G. Pennington, M.J. Mehl, Phys. Rev. B 76 (2006) 121405(R).
[24] Y.-W. Son, M.L. Cohen, S.G. Louie, Nature 444 (2006) 347.
[25] X.-F. Wang, T. Chakraborty, Phys. Rev. B 75 (2007) 033408.
[26] Y. Yao, F. Ye, X.L. Qi, S.C. Zhang, Z. Fang, Phys. Rev. B 75 (2007) 041401(R).
[27] C.L. Kane, E.J. Mele, Phys. Rev. Lett. 95 (2005) 226801.
[28] H. Min, J.E. Hill, N.A. Sinitsyn, B.R. Sahu, L. Kleinman, A.H. MacDonald, Phys. Rev. B 74 (2006) 165310.
[29] G.W. Semenoff, Phys. Rev. Lett. 53 (1994) 2449.
[30] K. Ziegler, Phys. Rev. B 53 (1996) 9653.
[31] V.P. Gusynin, S.G. Sharapov, J.P. Carbotte, Internat. J. Modern Phys. B 21 (2007) 4611.
[32] A. Bostowick, T. Ohta, J.L. McCesney, K.V. Emtsev, T. Seyller, K. Horn, E. Rotenberg, New J. Phys. 9 (2007) 385.
[33] S.Y. Zhou, G.H. Gweon, A.V. Federov, P.N. First, W.A. de Heer, D.H. Lee, F. Guinea, A.H. Castro Neto, A. Lanzara, Nature Mater. 6 (2007) 770.
[34] S.Y. Zhou, D.A. Siegel, A.V. Fedorov, A. Lanzara, Physica E 40 (2008) 2642.
[35] S.Y. Zhou, D.A. Siegel, A.V. Fedorov, A. Lanzara, Phys. Rev. Lett. 101 (2008) 086402.
[36] D.A. Siegel, S.Y. Zhou, F. El Gabaly, A.V. Fedorov, A.K. Schmid, A. Lanzara, Appl. Phys. Lett. 93 (2008) 243119.
[37] A. Grüneis, D.V. Vyalikh, Phys. Rev. B 77 (2008) 193401.
[38] A. Grüneis, K. Kummer, D.V. Vyalikh, arXiv: 0904.3220.
[39] G. Li, A. Luican, E.Y. Andrei, Phys. Rev. Lett. 102 (2009) 176804.
[40] G. Giovannetti, P.A. Khomyako, G. Brocks, P.J. Kelly, J. Van den Brink, Phys. Rev. B 76 (2007) 073103.
[41] H. Hiura, Appl. Surf. Sci. 222 (2004) 374;
J.C. Meyer, C.O. Girit, M.F. Crommie, A. Zettl, Appl. Phys. Lett. 92 (2008) 123110.
[42] B. Huard, J.A. Sulpizio, N. Stander, K. Todd, B. Yang, D. Goldhaber-Gordon, Phys. Rev. Lett. 98 (2007) 236803.
[43] C. Bai, X. Zhang, Phys. Rev. B 76 (2007) 075430.
[44] N. Abedpour, A. Esmailpour, R. Asgari, M.R. Rahimi Tabar, Phys. Rev. B 79 (2009) 165412.
[45] H. Sevinçli, M. Topsakal, S. Ciraci, Phys. Rev. B 78 (2009) 245402.
[46] A. Qaiumzadeh, R. Asgari, Phys. Rev. B 79 (2009) 075414;
A. Qaiumzadeh, F. Joubari, R. Asgari, arXiv: 0810.4681.
[47] S. Datta, Electronic Transport in Mesoscopic Systems, Cambridge University Press, 1995.
[48] N. Dombey, A. Calogeracos, Phys. Rev. 315 (1999) 41;
Paolo Christillin, Emilio d'Emilio, Phys. Rev. A 76 (2007) 042104.
[49] E.H. Hauge, J.A. Støvneng, Rev. Modern Phys. 61 (1989) 917.
[50] H.G. Winful, Phys. Rev. Lett. 91 (2003) 260401.
[51] Zhenhua Wu Kai, Chang Liu, J.T. Li, X.J. Chan, J. Appl. Phys. 105 (2009) 043702.